Protein and Ligand Environments of the S_2 State in Photosynthetic Oxygen Evolution: A Difference FT-IR Study†

Jacqueline J. Steenhuis and Bridgette A. Barry*

Department of Biochemistry, College of Biological Sciences, University of Minnesota, St. Paul, Minnesota 55108

Received: April 11, 1997; In Final Form: May 30, 1997⊗

Oxidation of water in photosynthetic organisms occurs in a chlorophyll containing enzyme, photosystem II. The catalytic manganese cluster of photosystem II cycles among five redox states called the S_n states. There are two forms of the S_2 state, which give rise to different EPR signals and which differ in magnetic coupling among the manganese atoms. We have used difference infrared spectroscopy to obtain more information about the environment of the manganese cluster in these two forms of the S_2 state. We present the 1600−1200 cm^{-1} region of the difference spectrum associated with the generation of the multiline state and the $g = 4.1$ S_2 state. The difference spectrum associated with generation of the S_2 multiline state from the dark stable S_1 state shows broad spectral features in the 1500−1200 cm^{-1} region at 1490 (negative), 1331 (negative), 1393 (positive), and 1267 (positive) cm^{-1}. Global ^{15}N labeling has little impact on intensities or frequencies in this region of the spectrum. These vibrational features are not observed in manganese-depleted, EDTA-treated photosystem II. Also, these features are not observed in oxygen-evolving photosystem II upon illumination at 80 K, a temperature where the manganese cluster is not oxidized. We conclude that these lines arise from amino acid residues that are close to or ligating to the cluster. From the frequencies and the lack of sensitivity to ^{15}N labeling, we favor the assignment of these lines to the asymmetric and symmetric stretch of one or more glutamate and/or aspartate residue(s). The spectral breadth of the lines is consistent with either an inhomogeneous or a homogeneous broadening mechanism. When illumination conditions are used that generate the $g = 4.1$ S_2 EPR signal, these vibrational lines are not observed. These results are discussed in terms of current models for the catalytic site.

Photosynthesis is the biological process by which light energy is converted to chemical energy. In plants, green algae, and prokaryotic cyanobacteria, two photosystems cooperate to transfer electrons from water to $NADP^+$. Photosystem II is the chlorophyll-containing reaction center that carries out the light-driven oxidation of water and reduction of plastoquinone. Photoexcitation of the primary chlorophyll donor, P_{680}, results in electron transfer from the excited singlet state of this molecule to a plastoquinone, called Q_A, on the "acceptor" side of the enzyme. A pheophytin molecule acts as an intermediate in this electron-transfer reaction. Q_A reduces Q_B, which will function as a two-electron and two-proton acceptor upon a subsequent charge separation. On the donor side, the chlorophyll cation radical, P_{680}^+, oxidizes a tyrosine residue, Z. The tyrosine radical, $Z^\bullet$, in turn oxidizes the active site. The active site of water oxidation contains a multinuclear metal cluster, which consists of four manganese atoms. The catalytic cycle of water oxidation involves five oxidation states called the Joliot−Kok S_n states, where n is the number of oxidizing equivalents stored at the active site. Four photons and four subsequent charge separations are necessary to complete one cycle at the active site. Each cycle results in the oxidation of two water molecules to form one molecule of oxygen and four protons. Photosystem II also contains a second redox active tyrosine, D, and a non-heme ferrous ion. The functions of this redox active tyrosine and the non-heme iron are yet to be elucidated (see, for example, reviews in refs 1 and 2). A third redox active tyrosine, M, has also been observed in some site-directed mutants of photosystem II.[3]

A structural model for the manganese cluster has been proposed based on XANES and EXAFS data.[4] In this model, four manganese atoms are arranged in two bis-μ-oxo bridged dimers. These dimers are linked at one side by two bridging carboxylato ligands and one μ-oxo bridge to form a C-shaped tetranuclear metal center. In addition, this model features one proximal calcium and one halide atom. However, as discussed, other possible structures are also consistent with the EXAFS data.[4] For representative examples of XANES and EXAFS experiments on photosystem II from other groups, see ref 5. Site-directed mutagenesis studies[6−8] suggest that the manganese atoms are coordinated by aspartate and glutamate residues. Study of manganese model compounds shows that such coordination will stabilize high oxidation states of the manganese cluster.[9] Such stabilization is a requirement for enzymatic efficiency. In addition, ESEEM studies of the S_2 state and ^{15}N labeling of histidine in photosystem II have provided evidence for coordination of manganese atoms by one or more histidine ligands.[10]

EPR studies of the S states have focused on the S_2 state (for example, see ref 11). Dark adaptation sets the catalytic center to the S_1 state. The S_2 state can be trapped by illumination at temperatures below 200 K.[12] There are two EPR detectable forms of the S_2 state.[11] One form, called the multiline state, gives rise to an EPR signal centered at $g = 2.0$. Hyperfine couplings to Mn(III) and Mn(IV) are observed and have been measured using ^{55}Mn ENDOR spectroscopy.[13] The second form of the S_2 state, called the $g = 4.1$ state, gives rise to a signal at lower field;[14,15] this signal exhibits no hyperfine splittings in untreated samples.[16] Recent Q band EPR studies on the $g =$

* To whom correspondence should be addressed. Address: Department of Biochemistry, 1479 Gortner Ave, University of Minnesota, St. Paul, MN 55108. Phone: 612-624-6732. Fax: 612-625-5780. E-mail: barry@biosci.cbs.umn.edu.

† Supported by a grant from the National Science Foundation, MCB 94-18164.

⊗ Abstract published in *Advance ACS Abstracts,* July 15, 1997.

S1089-5647(97)01260-1 CCC: $14.00

4.1 signal have provided evidence that there are two forms of the signal.[17] One form is produced in sucrose and shows non-Curie power saturation behavior. This signal has been assigned to an excited-state transition in the spin manifold from which the ground-state multiline signal arises.[18] The other spectral form is observed both in ethylene glycol and in glycerol, and the signal exhibits Curie law behavior above 4 K.[19,20] The origin of this signal is still under debate. It has been assigned either to a ground-state transition of a $S = {}^3/_2$ spin manifold[19] or to the middle Kramer's doublet of a $S = {}^5/_2$ spin manifold that has small zero-field splittings.[21,22] These two $g = 4.1$ signals were shown to have distinguishable line shapes at Q band frequencies.[17]

A diverse set of biochemical factors affect the ability to generate the $g = 4.1$ signal. These biochemical factors include the presence or absence of glycerol, ethylene glycol, sucrose, amines, and some anions (reviewed in ref 23). If glycerol or ethylene glycol is used as the cryoprotectant, illumination at 200 K generates the multiline form of the S_2 state, while illumination at 130 K produces the $g = 4.1$ form of the S_2 state.[15] Difference infrared studies have shown that the production of this signal is associated with a unique conformation of the protein backbone.[24] The rest of this work will focus on this $g = 4.1$ signal produced in glycerol. Interestingly, while a $g = 4.1$ signal has been observed in plant preparations, this signal has never been observed in cyanobacterial photosystem II preparations (reviewed in ref 25).

X-ray absorption studies have been performed on the form of the $g = 4.1$ state produced by 130 K illumination of glycerol-containing photosystem II membranes.[26,27] This work has shown that this state exhibits slightly different Mn−Mn distances when compared to the state exhibiting the multiline signal. A Mn−Mn distance of 2.7 Å was used to fit EXAFS data on the multiline form of the S_2 state. Two different distances of 2.7 and 2.8 Å for the two manganese dimers were used to fit the data for the $g = 4.1$ form of the S_2 state. Studies of model compounds[28,29] suggest that lengthening of the manganese−manganese distance could be caused by the protonation of one of the μ-oxo bridges of a manganese dimer. Protonation of the manganese dimer also increases the redox potential of the di-μ-oxo manganese model compounds and provides a possible means of accumulating oxidation equivalents without risking premature oxidation. Alternatively, the change in manganese−manganese distances could be caused by a change in coordination. This change in coordination must be facile enough to occur in the temperature range 130−200 K.[27]

The available evidence shows that the $g = 4.1$ and the multiline signals arise from an oxidation of the metal cluster to give a "S_2 state". The explanations for the origin of two EPR signals for this state can be divided into two groups. In the first set of explanations, the oxidized manganese is assumed to be the same metal atom in each S_2 state form. If the same metal ion is oxidized, then changes in magnetic coupling constants must underlie the observed spectral differences.[15,30] It has been proposed that the difference in magnetic coupling between the multiline and $g = 4.1$ state is mediated by protonation changes at a single μ-oxo bridge between the two dimer halves of the manganese cluster.[31] Alternatively, changes in ligation also have the potential to alter the type and magnitude of magnetic coupling, at least in binuclear manganese complexes.[32] In the second set of explanations, the identity of the oxidized species is proposed to be different in the two S_2 states.[17,33,34] For example, it has been proposed that the two signals arise from different sets of magnetically isolated manganese atoms in the tetranuclear cluster.[17,33]

We have used vibrational spectroscopy to obtain new information concerning the S_2 state. Difference infrared spectroscopy is a useful technique to apply, since it is sensitive to alterations in the ligand environment of the oxidized manganese cluster. We have previously published data in the 1800−1600 cm^{-1} region.[24] We now focus our attention on the 1600−1200 cm^{-1} region of the vibrational spectrum, which exhibits vibrational lines from amino acids in the vicinity of or ligating to the manganese cluster.

Materials and Methods

For experiments on plant photosystem II, a monodisperse photosystem II complex preparation,[35] with rates of oxygen evolution greater than 1000 μmol O_2 (mg chlorophyll h)$^{-1}$, was employed. The antenna size has been determined to be 100−120 chlorophylls per reaction center.[35,36] For some experiments, a photosystem II preparation from the cyanobacterium, *Synechocystis sp.* 6803, was used,[37,38] with rates of oxygen evolution equal to 2200 μmol O_2 (mg chlorophyll h)$^{-1}$. The antenna size of this preparation is approximately 55 chlorophylls per reaction center.[36,37] Both preparations contain low-potential cytochrome *b*-559.[39] Buffers for the plant photosystem II preparation (buffer A) contained 25% ultrapure glycerol, 50 mM MES−NaOH, pH 6.0, 7.5 mM $CaCl_2$, 240 mM NaCl, and 0.05% dodecyl maltoside (Anatrace, OH). Buffers used for the cyanobacterial photosystem II preparation contained 25% ultrapure glycerol, 50 mM MES−NaOH, pH 6.5, 20 mM $CaCl_2$, 300 mM NaCl, and 0.05% dodecyl maltoside (Anatrace, OH). To generate manganese-depleted samples, plant photosystem II preparations were treated with hydroxylamine by a procedure previously described.[38,40] To reduce binding of adventitious metals, manganese-depleted photosystem II samples were suspended in buffer A, which also contained 40 mM EDTA, pH 6.0. Oxygen evolution rates[38] were measured on samples immediately before spectroscopic experiments in order to verify that enzyme activities were preserved and were greater than the specific activity limits given above.

For ^{15}N labeling, the cyanobacterium, *Synechocystis sp*. PCC 6803, was employed. Cultures were grown in the presence of ^{15}N-nitrate (Cambridge Isotopes, MA). Isotopic incorporation was tested using mass spectrometry of chlorophyll.[42] ^{15}N incorporation into all four nitrogen atoms in acetone-extracted chlorophyll was found to be greater than 90%.

Although difference FT-IR studies often employ dehydrated or partially dehydrated samples in the absence of cryoprotectant (for example, see ref 35), the samples employed for these FT-IR and EPR experiments (and the experiments that we have previously reported[24]) contained water and glycerol.

Infrared spectra were recorded on a Nicolet 60-SXR spectrometer equipped with a liquid nitrogen-cooled MCT-B detector. Spectral resolution was 4 cm^{-1}, a Happ−Ganzel apodization function was used, double-sided interferograms were collected, mirror velocity was 1.57 cm/s, and 1000 mirror scans were coadded to construct each interferogram. The sample temperature was controlled to ±0.3 K with a High-Tran liquid nitrogen cryostat (R. G. Hansen & Associates, Santa Barbara, CA) and a temperature control unit (Scientific Instruments Model 9620, West Palm Beach, FL). The liquid nitrogen cryostat was equipped with CaF_2 windows. Illumination was provided with a Dolan-Jenner fiber optic annular illuminator equipped with a red filter and a heat filter. The absorbance of the amide I band at 1655 cm^{-1} was less than 0.9 absorbance unit. To construct the difference spectra, an interferogram recorded under illumination was ratioed directly to an interferogram recorded in the dark. Two to four of these difference

spectra were then averaged. Dark-minus-dark and light-minus-light spectra were also constructed and evaluated for each experiment. These spectra were found to be free of defined vibrational features. For presentation purposes, the difference spectra were corrected for the amplitude of the amide II band in the absorbance spectrum. Such a normalization is equivalent to a correction for protein concentration and path length. This is the only possible method of quantitative presentation of these FT-IR data, since small alterations in path length are not prevented by the design of the Hansen cryostat and sample holder. Comparison of infrared spectra obtained on EDTA-containing buffers with spectra obtained on non-EDTA-containing buffers showed that there was a negligible EDTA contribution at 1550 cm^{-1}.

EPR control experiments on the production of the S_2 state, of chlorophyll cation radicals, and of the Fe^{2+} Q_A^- signal were performed through the use of a Bruker EMX 6/1 EPR spectrometer equipped with an Oxford cryostat or as previously described.[24] An EPR spectrum was recorded in the dark before illumination. After illumination at the appropriate temperature, another EPR spectrum was recorded. A light-minus-dark difference spectrum was then generated. Saturating illumination was provided by a Dolan-Jenner illuminator equipped with both a red filter and a heat filter. Samples were illuminated out of the EPR cavity in a transparent, nitrogen-flow Dewar. The illumination at 200 K bath was performed in a dry ice−ethanol bath. The illumination at 130 K was performed by flowing cold nitrogen gas over the sample, and the illumination at 80 K bath was performed in a liquid nitrogen bath. Spectra were recorded at 4 K for the iron quinone signals or as described for chlorophyll cation radicals and the S_2 state signals.[24] Spin quantitations for chlorophyll cation and tyrosyl radical EPR signals were performed by double integration using the program IGOR or IGOR PRO (Wavemetrics, Lake Oswego, OR). Quantitation of iron quinone EPR signals was performed by measurement of the amplitude of the spectral feature at $g = 1.8$.

Spectral conditions for observation of the S_2 state signals were as described, except that in some experiments, the temperature was 10 K, the frequency was 9.44 GHz, the time constant was 328 ms, and the sweep time was 6 min.[24] Spectral conditions for observation of chlorophyll radical signals using a Varian E4 EPR spectrometer were as follows: microwave frequency, 9.1 GHz; microwave power, 0.4 mW; modulation amplitude, 3.2 G; scan time, 4 min; time constant, 2 s. Spectral conditions for observation of the iron quinone signals using a Bruker EMX 6/1 spectrometer were as follows: microwave frequency, 9.44 GHz; microwave power, 40 mW; modulation amplitude, 32 G; scan time, 11 min; time constant, 0.33 s. Multiple scans were collected to give a final spectrum that represents 40 min of data averaging.

Under some conditions, the non-heme iron atom in photosystem II can be oxidized to the ferric form (reviewed in Miller and Brudvig[23]). If this oxidation occurs, the non-heme iron atom can act as an electron acceptor. Our EPR spectra showed no evidence for the presence of a non-heme Fe^{3+} species in either the plant or the cyanobacterial photosystem II preparation employed here (data not shown).

Results

In Figure 1, we present cryogenic EPR control experiments on plant photosystem II samples. Upon illumination at 130 or 200 K, all S state transitions but S_1 to S_2 are blocked,[43] and electron transfer on the acceptor side of photosystem II is limited to reduction of the single electron acceptor, Q_A.[44] Thus,

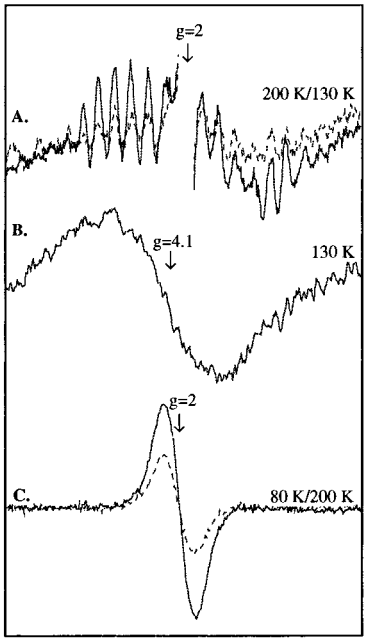

Figure 1. Light-minus-dark difference EPR spectra of donor side species in plant photosystem II. Spectrum A (depicted with a solid line) was obtained at 200 K and shows the multiline signal. The multiline spectrum obtained at 130 K is shown in the dotted line for comparison. Spectrum B was obtained at 130 K and shows the $g = 4.1$ signal. Spectrum C (depicted in the solid line) was obtained at 80 K and shows a chlorophyll cation radical signal. The chlorophyll cation radical signal obtained at 200 K is shown in the dotted line for comparison. Spectral line shapes are presented on arbitrary axes, and the peak-to-trough splitting for spectra A, B, and C is 710, 360, and 9 G, respectively. See Materials and Methods for other spectral conditions.

illumination of dark-adapted preparations at 200 and 130 K should result in production of the S_2 state and Q_A^-. At 200 K, the predominant signal originates from the multiline S_2 state.[15,24,45] At 130 K, the predominant signal originates from the $g = 4.1$ S_2 state.[15,24,45] Upon illumination at 80 K, the manganese cluster cannot be oxidized. Instead, in the photosystem II preparation employed here, chlorophyll is oxidized and Q_A is reduced. The chlorophyll cation radical contribution decreases as the temperature is raised from 80 K; the S_2 state contribution increases proportionally.[15,24,45] Cytochrome *b*-559, which could act as a donor at 80 K, is low potential and already oxidized in the photosystem II preparation employed here, so it does not contribute to light-minus-dark difference spectra.[39]

The data shown in Figure 1 are light-minus-dark EPR spectra constructed after illumination at 200 K (Figure 1A, solid line), 130 K (Figure 1B), and 80 K (Figure 1C, solid line). The signals produced on the donor side of photosystem II are shown. These data show that, as expected, the only donor side signal produced by illumination at 80 K is a chlorophyll radical (Figure 1C, solid line). The predominant donor side signal produced at 130 K is the $g = 4.1$ signal (Figure 1B). Only a low-amplitude multiline signal is produced upon 130 K illumination (Figure 1A, dotted line). The predominant signal at 200 K is the multiline signal (Figure 1A, solid line). At 200 K, in addition to the multiline signal, a $g = 4.1$ signal is also produced upon illumination, but its magnitude is less than one-half the magnitude of the $g = 4.1$ signal produced at 130 K.[24]

Spin quantitation of EPR chl^+ signals shows that in this plant preparation, 0.77 ± 0.06 chl^+ spin per reaction center (or per tyrosyl radical $D^\bullet$) is produced at 80 K (Figure 1C, solid line), while 0.33 ± 0.09 chl^+ spin per reaction center (or per tyrosyl radical $D^\bullet$) is produced at 200 K (Figure 1C, dotted line).

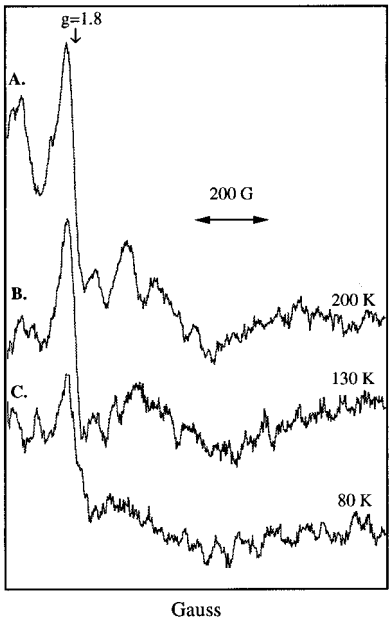

Figure 2. Light-minus-dark difference EPR spectra of acceptor side species in plant photosystem II. Spectra A, B, and C were obtained upon illumination at 200, 130, and 80 K, respectively. The spectra show the characteristic line shape of the $Fe^{2+}Q_A^-$ EPR signal. These signals are presented on the same *x* and *y* axes to aid in comparison. Samples contained 1.5 mg/mL chlorophyll. Note that spectra were obtained on relatively dilute samples in order to facilitate comparison of the results of illumination of EPR and FT-IR samples. See Materials and Methods for other spectral conditions.

Additional measurements (for example, six instead of three) have led us to revise the standard errors previously reported in these measurements; there has been no significant change in the average value, however.[24] At 130 K, 0.59 ± 0.08 chl^+ spin per reaction center (or per tyrosyl radical $D^\bullet$) is produced.

In Figure 2, we present EPR signals from the acceptor side of photosystem II. This broad signal arises from spin coupling between the reduced quinone, Q_A, and the ferrous ion found in photosystem II.[46,47] Several different types of $Fe^{2+}Q_A^-$ signals have been observed in plant and cyanobacterial preparations.[46,48,49] For example, a signal with a turning point at $g = 1.8$ has been reported; this signal has a negative component at $g = 1.67$.[23] The intensities of these signals are assumed to be proportional to the amount of Q_A^- formed under illumination and are assumed to reflect the extent of charge separation in photosystem II.[15,45]

The data presented in Figure 2 show that the iron quinone signal in the plant preparation employed exhibits a turning point at a *g* value of 1.8. The characteristic broad negative feature at higher field is also observed. There is no significant change in line shape as a function of illumination temperature. Apparent spectral differences between data recorded at 200 and 80 K (spectra A and C of Figure 2) are due to the observation of a small amount of multiline signal, which is mainly saturated at the high modulation amplitudes and microwave powers used to acquire the iron quinone signals. Averaging of replicate measurements shows that the amplitude of the $Fe^{2+}Q_A^-$ signal is approximately constant (±15%, average of six measurements) upon illumination at 200, 130, and 80 K, in agreement with earlier measurements.[15,45] Our experiments reflect the maximum possible contribution from Q_A^-, since only one equivalent of potassium ferricyanide is used to preoxidize the acceptor side. These experiments show that the extent of charge separation is constant at all three illumination temperatures.

In Figure 3, we present difference FT-IR spectra of plant photosystem II particles at 200 K (Figure 3A), 130 K (Figure 3B), and 80 K (Figure 3C). The base line is shown as the dotted line; this base line was extrapolated from the 1900−1800 cm^{-1} region, which has no infrared absorption. These data show the vibrational spectra associated with formation of the S_2 multiline state (Figure 3A) and the S_2 $g = 4.1$ state (Figure 3B) and with the oxidation of chlorophyll (Figure 3C). Since these are difference spectra, unique vibrational modes of S_2 will be positive lines and unique vibrational modes of S_1 will be negative lines. The terminal electron acceptor is the single electron acceptor, Q_A, as shown above. Therefore, each spectrum will also contain positive contributions from Q_A^- and negative contributions from Q_A. The intensities of spectral features from the acceptor side are expected to be constant at all three temperatures of illumination, as shown by our EPR control experiments (Figure 2). The nature of the plastoquinone contributions[50,51] to these spectra is under investigation in this laboratory, and we will discuss them in a forthcoming publication. There are no ferricyanide or ferrocyanide contributions to any region of the difference infrared spectrum, since only one equivalent of ferricyanide is used to preoxidize the acceptor side.

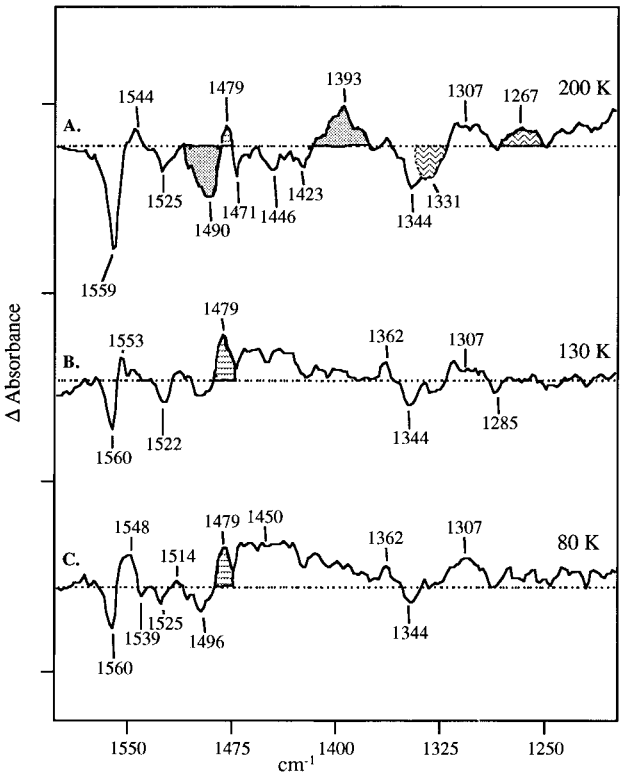

Figure 3. Light-minus-dark difference FT-IR spectra of plant photosystem II complexes obtained at (A) 200 K, (B) 130 K, and (C) 80 K. Data are averages of three or four difference spectra obtained from different samples. The tick marks on the *y* axis represent a Δ*A* of 0.002. The base line is extrapolated from the 1900−1800 cm^{-1} region, where there is no infrared absorbance. The hatch marks emphasize lines assigned in the text to chlorophyll (straight lines), to the asymmetric OCO stretch of a glutamate/aspartate(s) (solid fill), and to the symmetric OCO stretch of a glutamate/aspartate(s) (wavy lines). Spectral conditions are given in the Materials and Methods section.

Based on our EPR control experiments (described above), differences between the three spectra can be assigned to the donor side of photosystem II. As temperature increases, contributions to the spectrum from a chlorophyll cation radical should decrease and contributions from the manganese cluster will increase. For example, through the use of hydroxylamine-treated preparations and based on a 2 cm^{-1} ^{15}N shift, a positive line at 1479 cm^{-1} (positive) has been assigned to a chlorophyll macrocycle vibration in cyanobacterial photosystem II.[40,51] As

expected, the amplitude of the positive 1479 cm^{-1} line appears to decrease when spectra obtained at 80 and 200 K (spectra A and C of Figure 3) are compared. At 130 K (Figure 3B), this spectral feature appears to broaden. This could be caused by overlapping positive contributions in this spectral region. Redox active tyrosine radicals in photosystem II also make a potential contribution in this spectral region.[52] However, tyrosine $Z^{\bullet}$ is not stably oxidized in an oxygen-evolving preparation at this temperature.[53] Tyrosine $D^{\bullet}$ is already oxidized in our preparations and therefore does not contribute significantly to the light-minus-dark spectra (see, for example, Figure 1C).

Inspection of infrared spectra obtained at 200 K (Figure 3A) shows that production of the multiline S_2 state at 200 K is associated with unique, broad negative features at 1490 and 1331 cm^{-1} and with unique, broad positive lines at 1393 and 1267 cm^{-1}. The new feature at 1331 cm^{-1} overlaps with a negative line at 1344 cm^{-1}. Notice that these vibrational lines are among the most intense features in the difference spectrum. These spectral features are not observed when a chlorophyll cation radical (Figure 3C, 80 K) or predominantly the $g = 4.1$ EPR signal (Figure 3B, 130 K) is produced instead of the multiline S_2 signal. By contrast, intensities and frequencies of vibrational lines in the amide I region (1650 cm^{-1}) of the difference infrared spectrum are relatively unaffected, when spectra obtained at 80 and 200 K are compared.[24]

To gain more insight into the origin of the vibrational bands in the 1500−1200 cm^{-1} region of the spectrum, the plant photosytem II preparation was manganese-depleted. Illumination of this preparation at 200 K should produce chl^{+} and Q_A^{-}. EPR control experiments show that the magnitude of the $Fe^{2+}Q_A^{-}$ signal, produced upon 200 K illumination, is approximately the same when the manganese-depleted preparation is compared to the oxygen-evolving preparation. The magnitude of a 10 G EPR signal, previously assigned to a chlorophyll cation radical, increases upon this treatment (data not shown).

In Figure 4, we present a comparison of difference FT-IR spectra obtained upon illumination at 200 K in oxygen-evolving, manganese-containing (Figure 4A) and manganese-depleted (Figure 4B) plant preparations. These data show that manganese depletion results in a decrease in intensity of spectral features at 1490 (negative), 1331 (negative), 1393 (positive), and 1267 (positive) cm^{-1}. The spectrum obtained on manganese-depleted photosystem II is similar but not identical with spectra obtained on manganese-containing photosystem II at 80 K; spectral differences are observed in the 1750−1700 cm^{-1} region[24] and in the amide I and amide II (1550 cm^{-1}) regions. Comparison of spectra A and B of Figure 4 argues against an attribution of spectral features in the 1400−1200 cm^{-1} region of the S_2 multiline-minus-S_1 state to a chlorophyll radical or to Q_A^{-} and supports the assignment of these features to amino acids on the donor side of photosytem II.

Cyanobacterial photosystem II was then employed in these studies, since isotopic labeling is possible using this prokaryotic organism. Since both plants and cyanobacteria oxidize water by similar mechanism, any spectral features important for water oxidation should be observed in both preparations. As previously described, illumination of a cyanobacterial photosystem II preparation at 200 K produces a multiline signal.[24] An iron quinone signal and a chlorophyll cation radical EPR signal are also produced upon illumination at this temperature in the cyanobacterial preparation (data not shown).

In Figure 4, we present a comparison of difference FT-IR spectra of plant (Figure 4A) and cyanobacterial (Figure 4C) photosystem II preparations. Both sets of data were obtained at 200 K. Observed spectral differences between infrared data

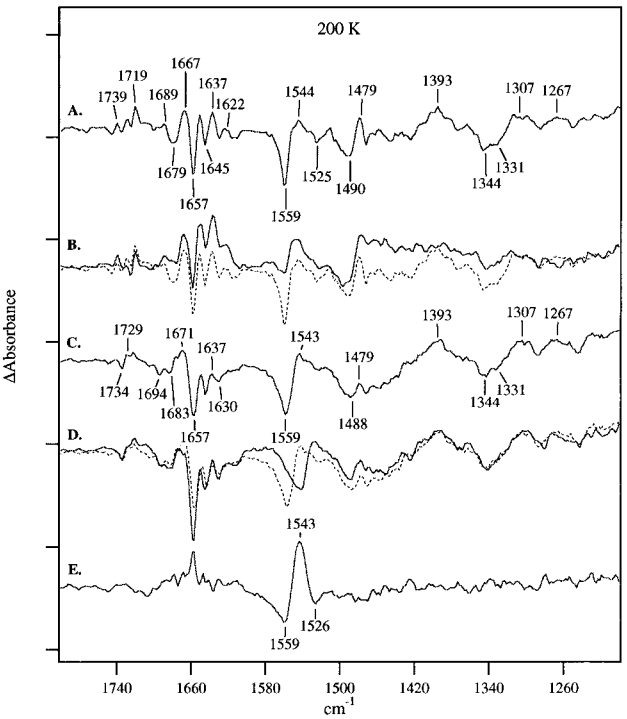

Figure 4. Light-minus-dark difference FT-IR spectra plant (spectra A and B) and *Synechocystis* 6803 (spectra C, D, and E) photosystem II illuminated at 200 K. Spectra were obtained from oxygen-evolving plant preparations (A), manganese-depleted plant preparations (B), oxygen-evolving cyanobacterial preparations (C), and globally ^{15}N-labeled cyanobacterial preparations (D). In spectrum E, we present the double difference ^{14}N-minus-^{15}N (spectrum C-minus-spectrum D). To ease comparison, spectrum A has been replicated as the dotted line in spectrum B, and spectrum C has been replicated as the dotted line in spectrum D. Data are averages of two to four individual difference spectra obtained on different samples. The tick marks on the *y* axis represent a ΔA of 0.002. Spectral conditions are given in the Materials and Methods section.

obtained from plant and cyanobacterial photosystem II probably reflect protein sequence differences. For example, note the changes in the 1750 cm^{-1} region, when Figures 4A and C are compared. The ester and keto vibrational modes of chlorophyll contribute in this region, as well as the carbonyl stretches of glutamic and aspartic acid residues.[51] Also, note that the spectral feature at 1479 cm^{-1} is superimposed on a broader, more intense negative feature in the cyanobacterial spectrum.

Infrared spectra obtained both from plant and from cyanobacterial photosystem II show spectral features at approximately 1490 (negative), 1331 (negative), 1393 (positive), and 1267 (positive) cm^{-1}. This result supports the interpretation that these features arise from amino acid residues in the environment of the manganese cluster, which are important and, therefore, conserved in water oxidation. Since we are acquiring difference spectra, these vibrational lines arise from the subset of ligating or neighboring residues that are perturbed upon oxidation of the catalytic site to form the multiline S_2 state.

The assignment of these vibrational features is of interest. Histidine is known to provide ligation for the manganese cluster.[10] Site-directed mutagenesis suggests that glutamate and aspartate residues provide ligation as well.[6−8] In Figure 4D (solid line), we present the spectrum obtained after global ^{15}N labeling of cyanobacterial photosystem II. A double difference spectrum, ^{14}N-minus-^{15}N, is shown in Figure 4E. Such labeling has the effect of substituting every nitrogen atom in the enzyme with the isotopee ^{15}N (see Materials and Methods). Vibrational modes that involve the movement of nitrogen atoms should be downshifted in frequency. For example, Figure 4D shows that

a differential feature at 1559 (negative)/1543 (positive) cm^{-1} downshifts 15 cm^{-1} upon ^{15}N labeling (spectra D and E of Figure 4). The frequencies and magnitude of the isotopic shift support the assignment of these two features to an amide II vibration.[54] This result is in agreement with our previous conclusion[24] that at 200 K, charge separation affects the magnitude of vibrational coupling constants, giving rise to amide I and amide II contributions (on the order of 10^{-3} absorbance units) in the difference infrared spectrum.

In the spectral region from 1700 to 1600 cm^{-1}, small ^{15}N-induced changes in intensity and frequency are also observed (see double difference spectrum, Figure 4E). The origin of these changes is under investigation. The amide I C═O vibration, which occurs in this spectral region, is expected to be relatively ^{15}N insensitive.[54] There may be small glutamine or asparagine contributions in this region.[55]

Compared to the signal-to-noise ratio, there are no dramatic changes upon ^{15}N labeling in the 1500−1200 cm^{-1} region (see spectra D and E of Figure 4). Note that, in our previous studies of photosystem II in the presence of hydroxylamine, the 1479 cm^{-1} line from chlorophyll showed a 2 cm^{-1} ^{15}N shift.[51] In these samples, the amplitude of this spectral feature is very low, and a 2 cm^{-1} shift cannot be resolved above the signal-to-noise (Figure 4E). The lack of clear ^{15}N shifts in the 1500−1200 cm^{-1} region argues against a well-defined amide III contribution to the difference spectrum, since this vibration should show some ^{15}N sensitivity. As discussed above, amide I and amide II contributions to the spectrum *are* observed. However, such an observation does not necessarily require an intense, accompanying amide III contribution to the difference spectrum, since the frequency of the amide III vibration is much more dependent on side chain composition.[54]

The lack of ^{15}N sensitivity also argues against imidazole ring contributions to the difference spectrum. Ring vibrations of histidine are expected in the 1400−1200 cm^{-1} region, and the expected ^{15}N shifts are in the range 17−6 cm^{-1}.[35,56] Such shifts would be readily observable, given our signal-to-noise, spectral resolution, and the precision to which the peak positions are known in FT-IR techniques. For example, note that the 15 cm^{-1} change in the amide II lines is clearly resolved in our data. This result argues against a contribution to the difference spectrum from imidazole groups bound to the manganese cluster. In turn, this result shows that oxidation of the metal cluster to form the S_2 multiline state does not perturb the ring stretching modes of histidine ligand(s) to the manganese cluster.[10] This result may imply that this histidine(s) is/are not ligated to the manganese atom that undergoes oxidation at 200 K. Alternatively, since the ring stretching modes of imidazole ligands are relatively insensitive to the nature of the bound metal ion,[57] it may be that the oxidation-induced shift in the histidine vibrational spectrum is too small to be detected in the 1500−1200 cm^{-1} region. We will undertake a study of model compounds with imidazole coordination in order to evaluate these possibilities.

The data in Figure 3 show that the vibrational spectrum associated with the production of the $g = 4.1$ signal (at 130 K) is also distinct from the vibrational spectrum associated with the production of the multiline state. In the 1600−1200 cm^{-1} region, the vibrational spectrum of the $g = 4.1$ state (Figure 3B) has a smaller number of positive and negative features, which serve to distinguish the spectrum from data recorded at 80 K (Figure 3C). Small spectral features that distinguish the 130 K difference spectra from data obtained at 80 K are observed in the spectral regions near 1550 and 1450 cm^{-1}. Our previous FT-IR studies have shown that difference spectra generated at 130 and 80 K show substantial changes in the amide I region, so the lack of alterations in this lower frequency region is not due to failure to produce the S_2 $g = 4.1$ state. This last conclusion is also supported by the EPR control experiments shown in Figure 1. The lack of alterations is also not due to a difference in the amount of charge separation, as assessed by the intensity of the iron quinone EPR signal (Figure 2). The difference infrared spectra shown in Figure 3 suggest that illumination at 130 K has a less dramatic effect on amino acid side chains that are in the vicinity of or ligating to the manganese cluster, when compared to production of the S_2 multiline state.

Discussion

We have used difference infrared spectroscopy to obtain structural information about the manganese cluster of photosystem II. We present here the 1600−1200 cm^{-1} region of difference infrared spectra: from the S_2 (multiline) Q_A^--minus-S_1 Q_A (200 K), S_2 ($g = 4.1$) Q_A^--minus-S_1 Q_A (130 K), and chl^+ Q_A^--minus-chl Q_A (80 K). In the spectrum associated with the formation of the S_2 multiline state, the region from 1500 to 1200 cm^{-1} shows two broad, intense negative features and two broad, intense, positive features. These lines, at 1490 (negative), 1331 (negative), 1393 (positive), and 1267 (positive) cm^{-1}, are only observed upon production of the S_2 multiline state and are not observed upon production of the S_2 $g = 4.1$ state at 130 K. The spectrum associated with production of the S_2 multiline state is similar in both oxygen-evolving plant and oxygen-evolving cyanobacterial photosystem II particles. Removal of the manganese cluster through hydroxylamine and EDTA treatment eliminates these spectral features. Furthermore, these vibrational lines are not observed upon oxidation of chlorophyll and reduction of Q_A at 80 K. EPR experiments predict that the Q_A^-/Q_A contribution is similar under all these conditions. These experiments rule out an assignment of features in the 1500−1200 cm^{-1} region to the acceptor side of photosystem II or to a chlorophyll cation radical in photosystem II. Therefore, we assign these spectral features to amino acid residues that are either close to or ligating to the manganese cluster. The definitive assignment of these spectral features to a given type of amino acid residue will depend on eventual isotopic labeling of amino acids in photosystem II. However, from the frequencies of the lines (see below) and the observed lack of sensitivity to ^{15}N labeling, we favor the assignment of these features to ionized carboxylate groups.[55]

The conclusions presented here should be contrasted to our previous analysis of the 1800−1700 cm^{-1} region, which led to the conclusion that a *protonated* carboxylic acid group was perturbed upon formation of the S_2 state by a change in hydrogen bonding or a dielectric change.[24] Also, difference infrared spectra, acquired at 80, 130, and 200 K, all exhibited vibrational features in the amide I region of the spectrum. The amide I regions of the 80 and 200 K spectra were similar, indicating that the vibrational spectrum of the peptide backbone responds in a way similar to the generation of a chlorophyll cation radical or to the generation of a the S_2 multiline state. However, the amide I region of the 130 K spectrum was distinct. The magnitude of the change is consistent with a change in vibrational coupling constant for a small percentage of the peptide backbone in photosystem II. These data imply that the generation of the $g = 4.1$ state is associated with a unique protein conformation.[24] The normal coordinate called the "amide I" vibration is primarily a delocalized, coordinated C═O stretch of the peptide backbone.[54] However, the asymmetric and symmetric stretching vibrations of glutamates and aspartates, upon which we focus in this work, are expected to be localized vibrational modes.[54]

Since we are performing difference spectroscopy, negatively charged, unprotonated glutamate or aspartate residues will contribute to the spectrum only if the structure or environment of the amino acid is altered upon oxidation of the metal cluster. Such a perturbation would occur upon oxidation of the manganese cluster if glutamate or aspartate provides ligation to metal atoms in the manganese cluster. Alternatively, oxidation of the cluster might perturb the vibrational spectrum of nonligating glutamate and aspartate residues through an electrostatic mechanism if oxidation of the metal cluster is associated with accumulation of positive charge.

Group frequency assignments argue that the symmetric and asymmetric stretches of nonligating carboxylate anions appear in the 1650−1400 cm^{-1} spectral region.[58] The asymmetric stretch O−C−O^- is expected to be higher in energy and to have more infrared intensity when compared to the symmetric O−C−O^- stretch. Surveys of the alterations in asymmetric and symmetric stretching frequencies upon ligation of metals have been reported.[57,59] However, the most extensive information available concerns only mononuclear metal centers, with a more limited data set available on more complex compounds (see, for example, refs 60−62). For mononuclear compounds, the symmetric and asymmetric stretch of bidentate or bridging ligands occurs in the spectral region from 1600 to 1400 cm^{-1}.[57,59] A similar range was observed for bridging ligands in multinuclear manganese complexes.[60−62] For example, for carboxyl stretching frequencies in acetato metal complexes, the two stretching modes are split by 40−170 cm^{-1}.[57] The energy of this splitting depends both on the metal ion and on the nature of the metal ligands. For unidentate carboxylato ligands, the splitting is observed to be greater than 40−170 cm^{-1}, with the C═O mode at higher frequencies and the C−O stretching mode at lower frequencies.[57] However, these data may be of limited *quantitative* relevance to the manganese cluster of photosystem II, since the nuclearity of the cluster and the valence of the metal ions influence the splitting between the asymmetric and symmetric stretching modes.[62] Also, if the metal cluster has symmetry, observed vibrational modes will transform as irreducible representations in the molecular point group and the atomic displacement may involve nuclear motion in more than one ligand.

An analysis of the frequencies of the vibrational modes that are unique to the S_2 multiline-minus-S_1 spectrum is of interest. Figure 4 and our previous work[24] show that the 200 K difference spectrum exhibits no *unique* vibrational modes in the region from 1650 to 1550 cm^{-1} of similar or greater intensity compared with the lines observed in the 1500−1200 cm^{-1} region. Such a spectral feature might occur if the lines observed in the 1500−1200 cm^{-1} region are the symmetric stretching component of a carboxylate group that has an asymmetric stretching component at higher energy. On the basis of this observation, we favor the hypothesis that the spectral feature at 1490 (negative)/1393 (positive) cm^{-1} arises from a downshift of a vibrational mode (perhaps the asymmetric stretching component) that arises from one or more glutamate and/or aspartate residue(s). Similarly, we assign the spectral feature at 1331 (negative)/1267 (positive) cm^{-1} to a downshift of a vibrational mode (perhaps the symmetric stretching component) that arises from one or more glutamate or aspartate residue(s). The frequency shift is caused by oxidation of manganese to form the S_2 multiline state. Note that the frequencies of maximum and minimum intensity in the difference spectrum do not necessarily correspond to the frequencies of the lines in the S_1 and S_2 state but depend on the relative intensities and line width of the vibrational lines, as recently described.[62]

Three lines of evidence suggest that our infrared data are consistent with the affected, putative carboxylate(s) residue providing ligation to the metal cluster. First, the direction of the shift in these vibrational lines upon oxidation of the metal is consistent with ligation by the putative glutamate/aspartate residue(s). Oxidation of the metal should result in a strengthening and shortening of the oxygen−metal bonds and in an upshift of oxygen−metal stretching frequencies.[62,63] A downshift of the corresponding C−O vibration would then be expected. Second, the energy splitting between the asymmetric and symmetric modes is consistent with ligation (but see discussion above).[57,61,62] Third, the observed frequencies are significantly lower than the observed frequencies for free carboxylates or for carboxylates ligating mononuclear metal clusters. Such low frequencies would suggest a significant environmental perturbation of the carboxylate, which are consistent with direct ligation of the group to one or more high-valence manganese in a multinuclear manganese complex.[62] For example, an asymmetric stretching mode with a frequency of 1540 cm^{-1} has previously been observed for a carboxylate ligand of a dinuclear Mn(III)Mn(IV) complex. By contrast, dinuclear Mn(II)Mn(II) compounds exhibited a carboxylate ligand asymmetric stretch at 1636 cm^{-1} (see ref 62 and references therein).

Thus, based on the limited amount of model compound data available at this time, we conclude that the frequencies, the splittings, and the direction of the shift upon oxidation are consistent with observation of ligands of the metal cluster. However, we cannot rule out other possibilities, i.e., that oxidation of the metal has an electrostatic effect on the vibrational spectrum of a nonligating carboxylate.

The width of the lines in the 1500−1200 cm^{-1} region of the S_2 multiline-minus-S_1 state is of potential significance. Lines in this spectral region have line widths (at half height) of approximately 15−30 cm^{-1}, while lines in the 1600 cm^{-1} region have line widths less than 10 cm^{-1}. Vibrational lines may be broad because of an inhomogeneous or a homogeneous broadening mechanism. Inhomogeneous broadening would result if multiple carboxylates are ligated to the metal cluster, and each different microenvironment imposes a different frequency on the ligating residue. Alternatively, heterogeneity in structure may give rise to slightly different frequencies for the same ligand in different reaction centers. A second possible explanation for spectral broadening in the 1500−1200 cm^{-1} would be a homogeneous broadening mechanism. Homogeneous broadening could result from small conformational motions occurring on the time scale (picosecond to nanosecond) of the measurement.[64] This is a particularly intriguing possibility given the observation of carboxylate ligand rearrangement in methane monooxygenase[65,66] and ribonucleotide reductase[67−69] upon oxidation/reduction of their respective dinuclear iron clusters. It may be that such carboxylate rearrangement also occurs upon oxidation of the metal cluster of photosystem II.

Formation of both EPR-observable forms of the S_2 state involves oxidation of manganese.[26] A small change in manganese−manganese distance is observed between the two S_2 state forms.[27] Through difference FT-IR spectroscopy, we observe the perturbation of a glutamate/aspartate residue(s) upon production of the S_2 multiline state. There is no evidence for such a perturbation upon production of the S_2 $g = 4.1$ state. There are a limited number of ways to account for these observations. For example, an alteration in protonation state or hydrogen bonding, when the $g = 4.1$ is compared to that of the multiline signal, is difficult to reconcile with these data. A change in protonation or hydrogen bonding would cause shifts in vibrational frequencies. However, the S_2 $g = 4.1$ difference

spectrum does not show lines with altered frequencies but, instead, shows a decrease in the number of observed vibrational lines. This result is consistent with a substantial change in ligand environment of the oxidized manganese in the two forms of the S_2 state and could be obtained if the identity of the oxidized species is different in the two forms of the S_2 state. Since these reactions are occurring at cryogenic temperatures where long-range conformation rearrangements are unlikely, one possible explanation is that formation of the S_2 $g = 4.1$ states involves an oxidation of one manganese atom, while at higher temperatures, formation of the S_2 multiline state involves transfer of that oxidizing equivalent onto a different metal ion. This is consistent with EXAFS analysis if the geometry of the cluster is not affected by this alteration and is also consistent with the amide I spectral changes that we have previously described.[24]

This suggestion can be reconciled with previous explanations for the origin of the magnetic differences between the two S_2 state EPR signals. Our results are predicted by explanations in which the two signals are postulated to arise from different, magnetically isolated parts of the metal cluster.[17,33] On the other hand, our results are also reconcilable with the first set of explanations in which ligand rearrangements or deprotonation events are postulated to mediate the change in coupling constant, since these proposals do not rule out the migration of oxidizing equivalents from one part of the cluster to another.[16,31,32]

Alternatively, if the full amplitude of the $g = 4.1$ state arises from only a small percentage of reaction centers in the sample, it may be difficult to observe vibrational lines from this state if these spectral features are broad. The spin quantum number of the $g = 4.1$ state is not known, and therefore, an absolute spin quantitation of the signal has not been performed.

A previous temperature study of the S_2-minus-S_1 difference infrared spectrum has been reported.[70] A negative band at 1404 cm^{-1} was assigned to a protein structural change accompanying the S_1-to-S_2 transition. These studies were performed in sucrose-containing buffers, where the $g = 4.1$ and the multiline signals are both formed upon 200 K illumination. In later work on the S_1-to-S_2 transition by the same group,[71] negative bands at 1560 and 1403 cm^{-1} and positive bands at 1587 and 1364 cm^{-1} were assigned to ligands of the manganese cluster that are perturbed upon formation of the S_2 state. We do not observe these vibrational modes under our conditions. The previous experiments were performed in sucrose-containing buffers at 250 K in the presence of the inhibitor DCMU. Instead of continuous illumination, a single, saturating laser flash was used to induce charge separation. High concentrations (20 mM total) of potassium ferricyanide and potassium ferrocyanide were employed, and the pH was 5.5. Experiments were performed on photosystem II membranes, not the more purified monodisperse photosystem II preparation employed here. Our experience indicates that the conditions used by Noguchi and co-workers are not optimal for the observation of vibrational features from the manganese cluster. The origin of the differences between our spectral data and those previously obtained is under investigation.

Our results have provided evidence for a substantial alteration in protein and ligand environments with the $g = 4.1$ and the multiline forms of the S_2 state. Our future work will involve examination of site-directed mutants of photosystem II in order to assign spectral lines to particular sites in the enzyme. We will also carry out single-flash experiments at higher temperature in order to observe other S state transitions.

Abbreviations

chl	chlorophyll
DCMU	3-(3,4-dichlorophenyl)-1,1-dimethylurea
EDTA	ethylenediaminetetraacetic acid
EPR	electron paramagnetic resonance spectroscopy
ENDOR	electron nuclear double resonance spectroscopy
ESEEM	electron spin echo envelope modulation spectroscopy
EXAFS	extended X-ray absorption fine structure
FT-IR	Fourier transform infrared spectroscopy
HEPES	*N*-(2-hydroxyethyl)piperazine-*N*′-2-ethanesulfonic acid
MES	2-(*N*morpholino)ethanesulfonic acid
XANES	X-ray absorption near-edge spectroscopy

References and Notes

(1) Babcock, G. T. In *New Comprehensive Biochemistry: Photosynthesis*; Amesz, J., Ed.; Elsevier: Amsterdam, 1987; pp 125−158.

(2) Sauer, K.; Yachandra, V. K.; Britt, R. D.; Klein, M. P. In *Manganese Redox Enzymes*; Pecoraro, V. L., Ed.; VCH Publishers: New York, 1992; pp 141−175.

(3) Boerner, R. J.; Barry, B. A. *J. Biol. Chem.* **1993**, *268*, 17151−17154.

(4) Yachandra, V. K.; DeRose, V. J.; Latimer, M. J.; Mukerji, I.; Sauer, K.; Klein, M. P. *Science* **1993**, *260*, 675−679.

(5) George, G. N.; Prince, R. C.; Cramer, S. P. *Science* **1989**, *243*, 789−791. MacLachlan, D. J.; Hallahan, B. J.; Ruffle, S. V.; Nugent, J. H. A.; Evans, M. C. W.; Strange, R. W.; Hasnain, S. S. *Biochem. J.* **1992**, *285*, 569−576. Ono, T.-A.; Noguchi, T.; Inoue, Y.; Kusunoki, M.; Matsushita, T.; Oyanagi, H. *Science* **1992**, *258*, 1335−1337. Riggs, P. J.; Mei, R.; Yocum, C. F.; Penner-Hahn, J. E. *J. Am. Chem. Soc.* **1992**, *114*, 10650−10651.

(6) Vermaas, W.; Charite, J.; Shen, G. *Biochemistry* **1990**, *29*, 5325−5332.

(7) Boerner, R. J.; Nguyen, A. P.; Barry, B. A.; Debus, R. J. *Biochemistry* **1992**, *31*, 6660−6672.

(8) Nixon, P. J.; Diner, B. A. *Biochemistry* **1992**, *31*, 942−948.

(9) Pecoraro, V. L. *Photochem. Photobiol.* **1988**, *48*, 249−264.

(10) Tang, X.-S.; Diner, B. A.; Larsen, B. S.; Gilchrist, M. L.; Lorigan, G. A.; Britt, R. D. *Proc. Natl. Acad. Sci. U.S.A.* **1994**, *91*, 704−708.

(11) Dismukes, G. C.; Siderer, Y. *Proc. Natl. Acad. Sci. U.S.A.* **1981**, *78*, 274−278. Casey, J. L.; Sauer, K. *Biochim. Biophys. Acta* **1984**, *767*, 21−28.

(12) Styring, S.; Rutherford, A. W. *Biochim. Biophys. Acta* **1988**, *933*, 378−387.

(13) Randall, D. W.; Sturgeon, B. E.; Ball, J. A.; Lorigan, G. A.; Chan, M. K.; Klein, M. P.; Armstrong, W. H.; Britt, R. D. *J. Am. Chem. Soc.* **1995**, *117*, 11780−11789.

(14) Zimmermann, J.-L.; Rutherford, A. W. *Biochim. Biophys. Acta* **1984**, *767*, 160−167.

(15) de Paula, J. C.; Innes, J. B.; Brudvig, G. W. *Biochemistry* **1985**, *24*, 8114−8120.

(16) Kim, D. H.; Britt, R. D.; Klein, M. P.; Sauer, K. *J. Am. Chem. Soc.* **1990**, *112*, 9389- 9391.

(17) Smith, P. J.; Pace, R. J. *Biochim. Biophys. Acta* **1996**, *1275*, 213−220.

(18) Pace, R. J.; Smith, P. J.; Bramley, R.; Stehlik, D. *Biochim. Biophys. Acta* **1991**, *1058*, 161−170.

(19) de Paula, J. C.; Beck, W. F.; Brudvig, G. W. *J. Am. Chem. Soc.* **1986**, *108*, 4002−4009.

(20) Vanngard, T.; Hansson, O.; Haddy, A. In *Manganese Redox Enzymes*; Pecoraro, V. L., Ed.; VCH Publishers: New York, 1992; pp 105−118.

(21) Haddy, A.; Dunham, W. R.; Sands, R. H.; Aasa, R. *Biochim. Biophys. Acta* **1992**, *1099*, 25−34.

(22) Astashkin, A. V.; Kodera, Y.; Kawamori, A. *J. Magn. Reson., Ser. B* **1994**, *105*, 113−119.

(23) Miller, A.-F.; Brudvig, G. W. *Biochim. Biophys. Acta* **1991**, *1056*, 1−18.

(24) Steenhuis, J. J.; Barry, B. A. *J. Am. Chem. Soc.* **1996**, *118*, 11927−11932.

(25) Debus, R. J. *Biochim. Biophys. Acta* **1992**, *1102*, 269−352.

(26) Cole, J.; Yachandra, V. K.; Guiles, R. D.; McDermott, A. E.; Britt, R. D.; Dexheimer, S. L.; Sauer, K.; Klein, M. P. *Biochim. Biophys. Acta* **1987**, *890*, 395−398.

(27) Liang, W.; Latimer, M. J.; Dau, H.; Roelofs, T. A.; Yachandra, V. K.; Sauer, K.; Klein, M. P. *Biochemistry* **1994**, *33*, 4923−4932.

(28) Baldwin, M. J.; Gelasco, A.; Pecoraro, V. L. *Photosynth. Res.* **1993**, *38*, 303−308.

(29) Baldwin, M. J.; Stemmler, T. L.; Riggs-Gelasco, P. J.; Kirk, M. L.; Penner-hahn, J. E.; Pecoraro, V. L. *J. Am. Chem. Soc.* **1994**, *116*, 11349−11356.

(30) Zimmermann, J.-L.; Rutherford, A. W. *Biochemistry* **1986**, *25*, 4609−4615.

(31) Hagen, K. S.; Westmoreland, T. D.; Scott, M. J.; Armstrong, W. H. *J. Am. Chem. Soc.* **1989**, *111*, 1907−1909.
(32) Wieghardt, K. *Angew. Chem., Int. Ed. Engl.* **1989**, *28*, 1153−1172.
(33) Hansson, O.; Aasa, R.; Vanngard, T. *Biophys. J.* **1987**, *51*, 825−832.
(34) Boussac, A.; Girerd, J. J.; Rutherford, A. W. *Biochemistry* **1996**, *35*, 6984−6989.
(35) MacDonald, G. M.; Barry, B. A. *Biochemistry* **1992**, *31*, 9848−9856.
(36) Patzlaff, J. S.; Barry, B. A. *Biochemistry* **1996**, *35*, 7802−7811.
(37) Noren, G. H.; Boerner, R. J.; Barry, B. A. *Biochemistry* **1991**, *30*, 3943−3950.
(38) Barry, B. A. *Methods Enzymol.* **1995**, *258*, 303−318.
(39) MacDonald, G. M.; Boerner, R. J.; Everly, R. M.; Cramer, W. A.; Debus, R. J.; Barry, B. A. *Biochemistry* **1994**, *33*, 4393−4400.
(40) Bernard, M. T.; MacDonald, G. M.; Nguyen, A. P.; Debus, R. J.; Barry, B. A. *J. Biol. Chem.* **1995**, *270*, 1589−1594.
(41) Rippka, R.; Derulles, J.; Waterbury, J. B.; Herdman, M.; Stanier, R. *J. Gen. Microbiol.* **1979**, *111*, 1−61.
(42) Grese, R. P.; Cerny, R. L.; Gross, M. L.; Senge, M. *J. Am. Soc. Mass Spectrom.* **1990**, *1*, 72−84.
(43) Styring, S.; Miyao, M.; Rutherford, A. W. *Biochim. Biophys. Acta* **1987**, *890*, 32−38.
(44) Joliot, P.; Joliot, A. *Biochim. Biophys. Acta* **1973**, *305*, 302−316.
(45) de Paula, J. C.; Li, P. M.; Miller, A.-F.; Wu, B. W.; Brudvig, G. W. *Biochemistry* **1986**, *25*, 6487−6494.
(46) Nugent, J. H. A.; Diner, B. A.; Evans, M. C. W. *FEBS Lett.* **1981**, *124*, 241−244.
(47) Butler, W. F.; Calvo, R.; Fredkin, D. R.; Isaacson, R. A.; Okamura, M. Y.; Feher, G. *Biophys. J.* **1984**, *45*, 947−973.
(48) McDermott, A. E.; Yachandra, V. K.; Guiles, R. D.; Cole, J. L.; Dexheimer, S. L.; Britt, R. D.; Sauer, K.; Klein, M. P. *Biochemistry* **1988**, *27*, 4021−4031.
(49) Rutherford, A. W.; Zimmerman, J. L. *Biochim. Biophys. Acta* **1984**, *767*, 168−175.
(50) Hienerwadel, R.; Boussac, A.; Breton, J.; Berthomieu, C. *Biochemistry* **1996**, *35*, 15447−15460.
(51) MacDonald, G. M.; Steenhuis, J. J.; Barry, B. A. *J. Biol. Chem.* **1995**, *270*, 8420−8428.
(52) MacDonald, G. M.; Bixby, K. A.; Barry, B. A. *Proc. Natl. Acad. Sci. U.S.A.* **1993**, *90*, 11024−11028.
(53) Warden, J. T.; Blankenship, R. E.; Sauer, K. *Biochim. Biophys. Acta* **1976**, *423*, 462−478.
(54) Krimm, S.; Bandekar, J. In *Advances in Protein Chemistry*; Anfinsen, C. B., Edsall, J. T., Richards, F. M., Eds.; Academic Press: New York, 1986; Vol. 38, pp 181−364.
(55) Flett, M. S. C. *Spectrochim. Acta* **1962**, *18*, 1537−1556.
(56) Majoube, M.; Vergoten, G. *J. Mol. Struct.* **1992**, *266*, 345−352.
(57) Nakamoto, K. *Infrared and Raman spectra of inorganic and coordination compounds*; John Wiley & Sons: New York, 1986; pp 206−238.
(58) Bellamy, L. J. *The infrared spectra of complex molecules*; Chapman and Hall: London, 1980; Vol. 1, pp 183−202.
(59) Deacon, G. B.; Phillips, R. J. *Coord. Chem. Rev.* **1980**, *33*, 227−250.
(60) Sheats, J. E.; Czernuszewicz, R. S.; Dismukes, G. C.; Rheingold, A. L.; Petrouleas, V.; Stubbe, J.; Armstrong, W. H.; Beer, R. H.; Lippard, S. L. *J. Am. Chem. Soc.* **1987**, *109*, 1435−1444.
(61) Czernuszewicz, R.; Dave, B.; Rankin, J. G. In *Spectroscopy of Biological Molecules*; Hester, R. E., Girling, R. B., Eds.; Royal Society of Chemistry: Cambridge, 1991; pp 285−288.
(62) Smith, J. C.; Gonzalez-Vergara, E.; Vincent, J. B. *Inorg. Chim. Acta* **1997**, *255*, 99−103.
(63) Greenwood, N. N. *Spectroscopic properties of inorganic and organometallic compounds*; Chemical Society: London, 1968; pp 199−206.
(64) Flygare, W. H. *Molecular structure and dynamics*; Prentice-Hall, Inc: Englewood Cliffs, NJ, 1978.
(65) Rosenzweig, A. C.; Frederick, C. A.; Lippard, S. J.; Nordlund, P. *Nature* **1993**, *366*, 537−543.
(66) Rosenweig, A. C.; Nordlund, P.; Takahara, P. M.; Frederick, C. A.; Lippard, S. J. *Chem. Biol.* **1995**, *2*, 409−418.
(67) Nordlund, P.; Sjoberg, B.-M.; Eklund, H. *Nature* **1990**, *345*, 593−598.
(68) Nordlund, P.; Eklund, H. *J. Mol. Biol.* **1993**, *232*, 123−164.
(69) Logan, D. T.; Su, X. D.; Aberg, A.; Regnstrom, K.; Hajdu, J.; Eklund, H.; Nordlund, P. *Structure* **1996**, *4*, 1053−1064.
(70) Noguchi, T.; Ono, T.-a.; Inoue, Y. *Biochim. Biophys. Acta* **1993**, *1143*, 333−336.
(71) Noguchi, T.; Ono, T.-a.; Inoue, Y. *Biochim. Biophys. Acta* **1995**, *1232*, 59−66. Noguchi, T.; Ono, T.-a.; Inoue, Y. *Biochim. Biophys. Acta* **1995**, *1228*, 189−200.